Novel low-temperature synthesis and characterization of $LiNiVO_4$ for high-voltage Li ion batteries

S. R. S. Prabaharan,[a] M. S. Michael,[a] S. Radhakrishna[a] and C. Julien*[b]

[a]*Centre for Advanced Materials, Institute of Advanced Studies, University of Malaya, 50603 Kuala Lumpur, Malaysia*
[b]*Laboratoire des Milieux Désordonnés et Hétérogènes, Université Pierre et Marie Curie, 4, place Jussieu, 75252 Paris cedex 05, France*

A novel high-voltage cathode material, $LiNiVO_4$, with an inverse spinel structure, space group, $Fd\bar{3}m$ (O_h^7) has been synthesized at temperatures as low as 320 °C using the aqueous glycine–nitrate combustion process. The phase purity of the synthesized product has been found to be excellent as confirmed by X-ray diffraction and Raman spectroscopy. The physical grain size has been determined from SEM analysis. EDAX measurements indicate the presence of nickel and vanadium at the stoichiometric level. Thermal studies of the precursor show evidence for the phase formation and/or crystallization of the inverse spinel compound. The electrochemical behaviour of this compound, which is used as a positive electrode in lithium batteries, exhibits a high voltage of 4.8 V *vs.* Li and has been assessed by slow scan cyclic voltammetry in 2450 coin-type electrochemical test cells including a Li metal anode or a carbonaceous anode as well as a high voltage resistant organic non-aqueous mixed electrolyte. The cyclic voltammograms show excellent reversibility of the compound, proving its redox kinetics in lithium-containing rechargeable cells.

New lithiated transition-metal oxides, such as $LiNiVO_4$ and $LiCoVO_4$, have been recently proposed as cathode-active materials for modern rechargeable batteries. These materials are very attractive for their use in the so-called Li ion or rocking-chair batteries due to their theoretical capacity of about 148 mA h g^{-1}.[1] Apart from a capacity of about 45 mA h g^{-1} and a high potential of 4.8 V *vs.* Li^+/Li, very few details regarding their lithium insertion properties are presently known. Besides, the structure–property relationships concerning the structural and magnetic properties of these compounds have already been reported.[2] The crystal structure information has been known since 1961; they are inverse spinels giving rise to a three-dimensional network for Li ion diffusion.[3]

Fey *et al.*[1] have recently evaluated the redox behaviour of $LiNiVO_4$ and $LiCoVO_4$ as cathode-active materials in non-aqueous electrochemical cells. They have proved that the deintercalation/intercalation reaction involving the removal/insertion of Li^+ at potentials as high as *ca.* 4.8 V *vs.* Li^+/Li for the compound $LiNiVO_4$. These compounds were synthesized through solid-state reaction between their respective nitrates and oxides at a very high temperature, *ca.* 800 °C. This method has the obvious disadvantage that all solid particles may not react completely, leaving undesirable substances in the cathode material, as pointed out in a recent publication.[1] For instance, the final product $LiNiVO_4$ contains NiO impurities, which may affect the cycling properties and reduce its electrochemical features. Further, such impurities diminish the specific capacity of the electrode material when it is employed as a cathode in rechargeable lithium cells. In addition, the temperature of formation of this compound is quite high. These drawbacks can be overcome by employing a suitable low-temperature synthesis procedure. Recently, the preparation of lithiated transition-metal oxides for battery applications has been of considerable interest.[4–8] In the present work, we describe a simple procedure for the preparation of bulk quantities of submicron-sized particles of electrochemically active single-phase $LiNiVO_4$ at low temperature of 320 °C. This procedure is called the aqueous glycine–nitrate precursor method. From the present study, it has been proved that lithiated transition-metal oxides can be synthesized with high phase purity together with high product yield to be ultimately used as cathode-active material in lithium-containing rechargeable batteries.

Experimental

Synthesis procedure

Stoichiometric amounts of aqueous solutions of nitrates of lithium and nickel, and ammonium metavanadate, NH_4VO_3 (99.9% purity), were first dissolved in triple distilled water, and then mixed with glycine solution. The latter acts as a fuel for the spontaneous combustion of the mixed solution at elevated temperatures. The stoichiometric composition of glycine for the spontaneous decomposition of the mixtures was twice the molar fraction of total stoichiometry of the starting materials. The mixture solution was heated to boiling and underwent dehydration at 100 °C and a green–black sticky paste was obtained. The paste was then allowed to decompose at around 250 °C. The decomposition was accompanied by a mass of small bubbles (foams) followed by the generation of combustible gases such as NO_x and ammonia, which ultimately gave rise to a pale brown powder, referred to as the precursor. Further, as the process continued, the volatile combustible gases ignited as a result of the exothermic decomposition, yielding a voluminous black mass, and subsequently turned yellow. The origin of the colour change during this process is obviously due to oxidation of trivalent vanadium (V^{3+}) to pentavalent vanadium (V^{5+}).

Although the X-ray diffraction patterns confirm the formation of the desired phase of the final product $LiNiVO_4$ (see later), the content of amorphous material present at this stage ensures the need for further annealing. Accordingly, the powder mass was annealed at 350 and 500 °C in air for 6 h in order to improve the crystallinity of the $LiNiVO_4$ final product. A theoretical reaction, assuming complete thermal decomposition of the starting materials, may be written as:

$$LiNO_3(aq) + Ni(NO_3)_2(aq) + NH_4VO_3(aq) + 6NH_2CH_2COOH(aq) \xrightarrow{\text{heat}\downarrow\text{air}} LiNiVO_4(s) + 5N_2(g) + 12CO_2(g) + 17H_2O(g)$$

Fig. 1 shows a flow chart describing the procedure adopted for the synthesis of the crystalline $LiNiVO_4$ single phase.

Powders were first studied by several physical characterization techniques, such as powder X-Ray diffraction (XRD),

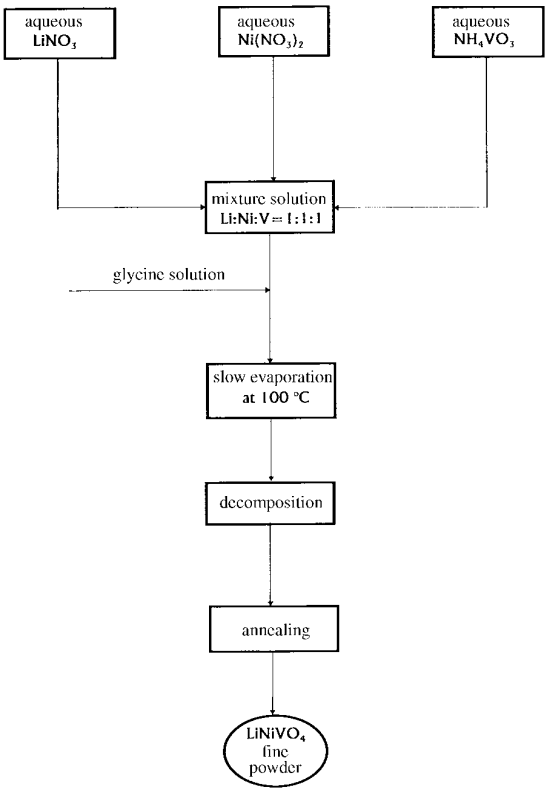

Fig. 1 Flow chart showing the low-temperature synthesis of single-phase $LiNiVO_4$

Raman and Fourier-transform IR (FTIR) spectroscopy, thermal analysis (TG and DTA), scanning electron microscopy (SEM) and energy dispersive analysis by X-rays (EDAX).

Phase analysis

XRD patterns were obtained either with a Philips model PW 1840/01/11 or a JEOL model JDX 8030 X-ray diffractometer using nickel-filtered Cu-Kα radiation. The diffraction patterns were taken at room temperature in the range of $10^\circ \leqslant 2\theta \leqslant 80^\circ$ using step scans. The step size and the scan rate were set at 0.1° and 2° min^{-1}, respectively.

Spectroscopic studies

Room-temperature Raman spectra were collected in the quasi-backscattering configuration on the powder sample annealed at 500 °C. A Jobin-Yvon model U1000 double monochromator with holographic gratings and a computer-controlled photon-counting system was used in conjunction with the 514.5 nm argon ion laser line. Spectra which are the average of 12 scans obtained with a spectral resolution of 4 cm^{-1}, were recorded using a low excitation power of 10 mW. FTIR spectra were recorded using a Brucker IFS 113v interferometer. The sample powders were well mixed in a KBr matrix.

SEM, EDAX and thermal analyses

SEM images were collected by employing a Philips scanning microscope (model 515) and the EDAX signals were recorded using an analyser attached to the scanning microscope. Thermal analyses of the precursor complex were performed simultaneously using a TG–DTA apparatus (Thermal Sciences model STA-1500). Experiments were carried out under ambient atmosphere with a heating rate of 10 °C min^{-1}.

Electrochemical studies

In order to test the Li^+ intercalation/deintercalation kinetics and to study the battery operation, the test cells were fabricated in both Li/$LiNiVO_4$ and C/$LiNiVO_4$ configurations using a non-aqueous Li^+ ion conducting organic electrolyte environment. Electrochemical cells were fabricated in our laboratory as follows. The composite cathode was built from the mixture of inverse spinel $LiNiVO_4$ powders (500 °C) (the electrochemically active materials), black carbon and PTFE binder. These components were mixed together in the mass ratio 85:10:5 and pressed on to an expanded aluminium microgrid (Delker Corporation, USA) at a pressure of 5 tonnes cm^{-2}. This procedure gives circular pellet electrodes of 20 mm diameter. The pellets were then dried at 120 °C in air. Similarly, the carbonaceous electrode was prepared using a natural graphite NG-7 (from Kansai Coke and Chemicals Co., Japan). The active material (NG-7) was mixed with the PTFE binder in the mass ratio 90:10 and pressed on to a copper mesh (Delker Co., USA) and subsequently dried at 120 °C. A microporous polypropylene membrane, Celgard 2400 (Hoechst Celanese Co., USA), was used as the separator between the cathode and the anode. Electrodes and separators were soaked in an appropriate electrolyte. The electrolyte was prepared by dissolving either 1 M $LiPF_6$ or 1.5 M $LiBF_4$ as electrolyte salt in a volume ratio 50:45:5 mixture of ethylene carbonate (EC), dimethyl carbonate (DMC) and methyl formate (MF). This electrolyte composition was found to be stable at voltages higher than 5.1 V[9] and, hence, employed in the present work as the electrolyte medium.

In the present study, we fabricated two types of test cells. The Li/El/$LiNiVO_4$ cell (cell 1) includes a negative electrode of Li metal pressed manually onto a copper expanded mesh and the inverse spinel composite powder as the positive electrode. The C/El/$LiNiVO_4$ cell (cell 2) is constituted of carbonaceous anode (NG-7 + PTFE binder) and the composite $LiNiVO_4$ cathode. These two cells were assembled inside a home-made glove box filled with purified argon whose humidity was maintained within 10% RH. The assembled cells were then hermetically sealed. These cells were fabricated either using a 2450 coin-type cell assembly or a Swage-lock-type two-electrode cell made up of PTFE walls whose inside dimensions are typically the same as those in the 2450 configuration. The cell cases were made with 316L corrosion-resistant stainless steel. The cells thus made were left for 24 h in order to test their open-circuit voltage (OCV). As a first step in assessing their cycling behaviour, the cyclic voltammograms were recorded at a slow scan rate in the potential range between 3.0 and 5.0 V using a BAS CV-27 apparatus.

Results and Discussion

Structural phase analysis

X-Ray diffraction analysis was carried out on the synthesized product at various preparation stages of the inverse spinel product $LiNiVO_4$ to monitor the phase purity and structure, phase concentrations and the amorphous content. Fig. 2 shows the XRD powder diagrams of precursor (curve a), decomposed product (curve b), and material calcined at 350 °C (curve c). Fig. 3 shows the X-ray diffractogram of the $LiNiVO_4$ compound annealed at 500 °C. This diffractogram reveals the formation of a highly crystalline phase of the product with high phase purity upon annealing. The diffraction peaks were indexed assuming the inverse spinel structure and the search match was obtained using a UPDSM-Release 4.25 program. The latter analysis provides a perfect fitting to the above XRD data with respect to the JCPDS record (38–1395) and evidently, there are no residues present in the diffractogram (see Fig. 4) proving that the product obtained in this study has a single-phase structure without any noticeable residual impurit-

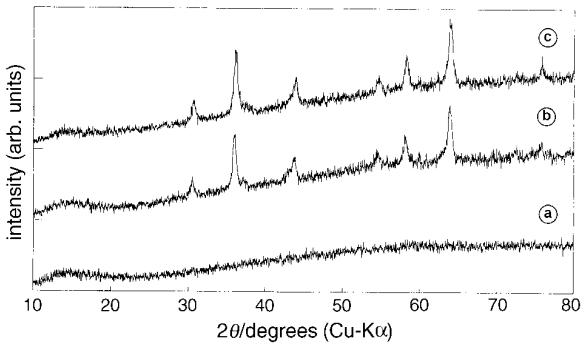

Fig. 2 X-Ray powder diffractograms for: (a) precursor, (b) decomposed product and (c) sample calcined at 350 °C

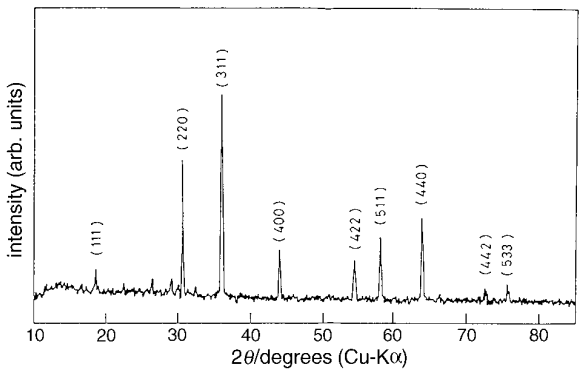

Fig. 3 Indexed XRD powder patterns of inverse spinel $LiNiVO_4$

ies. However, Fey *et al.*[1] have reported the presence of a NiO impurity peak at 43.5° in their $LiNiVO_4$ product prepared *via* a high-temperature solid-state reaction. The lattice constant of the single-phase product was measured to be 8.222 Å, which is in good agreement with the literature value of 8.2198 Å.[10]

Fig. 2 (a)–(c) shows the diffractograms obtained at various stages of preparation of the inverse spinel $LiNiVO_4$. As can be seen from these results, a completely amorphous structure is obtained for the precursor powder as expected [Fig. 4(a)]. However, the product obtained after the spontaneous combustion shows diffraction peaks [Fig. 4(b)] corresponding to $LiNiVO_4$ as confirmed by comparing with JCPDS data using UPDSM software. The compound still exhibits an amorphous background, although the overall diffraction spectrum agrees well with the published results. The domain size of the product annealed at 500 °C has been calculated to be 0.0382 μm using the full-width at half maximum (FWHM) data for the (311) peak located at about 36°.

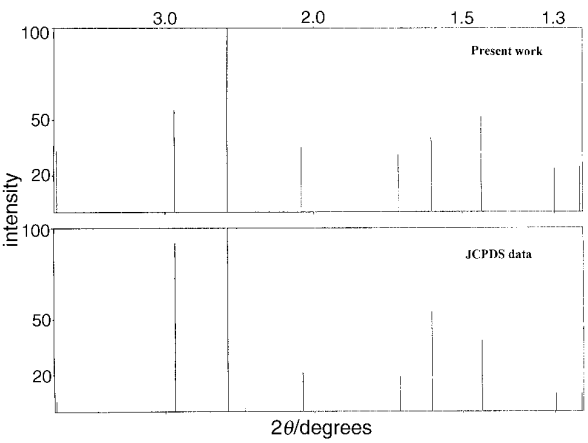

Fig. 4 JCPDS search match data obtained from UPDSM-software for inverse spinel $LiNiVO_4$

Vibrational spectroscopy

The cubic spinel structure possesses prototypic $Fd\bar{3}m$ (O_h^7) symmetry. The pentavalent vanadium is located on the tetrahedral (8a) sites, whereas Li and Ni are distributed on the octahedral (16d) sites, the distribution being disordered in the simple spinel structure[2] as shown in Fig. 5. Factor group theoretical analysis of spinel-type compounds yields nine optic modes allowed at the centre of the Brillouin zone

$$\Gamma = 1A_{1g} + 1E_g + 3F_{2g} + 4F_{1u}$$

in which five optic modes are Raman-active ($A_{1g} + E_g + 3F_{2g}$) and four are IR-active ($4F_{1u}$).[11–15]

Fig. 6 and 7 show the room-temperature Raman scattering and IR absorption spectra of single-phase $LiNiVO_4$ annealed at 500 °C, respectively. From these results, it can be observed that: (a) these spectra exhibit a complex pattern of broad bands in the 700–850 cm^{-1} region; (b) the high-frequency vibrational bands are the dominant ones; and (c) the IR spectrum shows some additional peaks which are not expected from group theory.

The high-frequency vibrational bands of a spinel can be assigned to a vibration between the oxygen and the highest-valency cation. Two vibrational modes, namely the stretching frequencies of the VO_4 tetrahedron, are expected to be observed in this region. Considering an isolated VO_4 tetrahedron, the

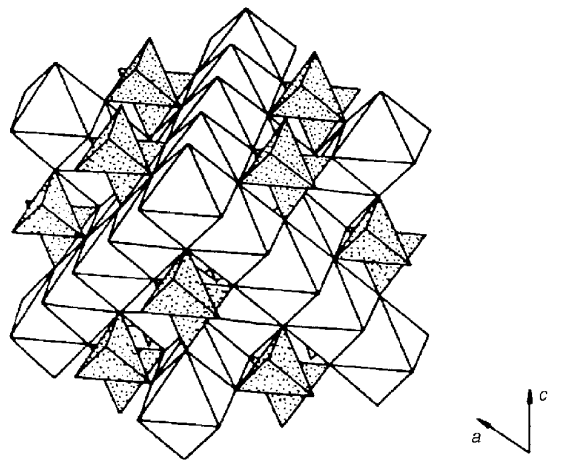

Fig. 5 Projection of the inverse spinel $LiNiVO_4$ structure along the [001] direction showing tetrahedra (shaded) and Li/Ni octahedra

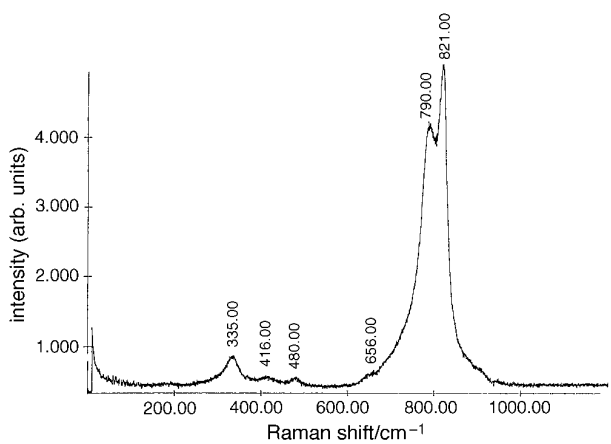

Fig. 6 Raman spectrum of inverse spinel $LiNiVO_4$ recorded at room temperature

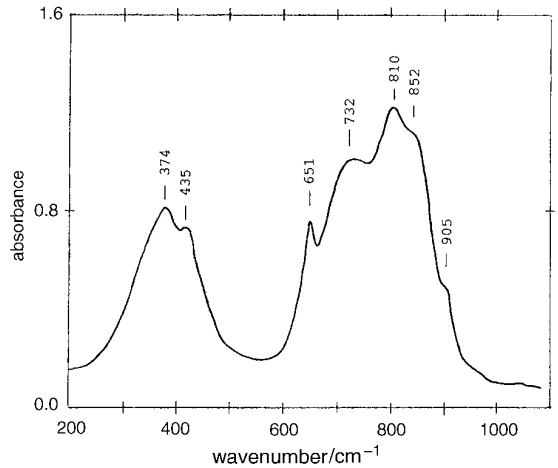

Fig. 7 FTIR spectrum of inverse spinel $LiNiVO_4$ recorded at room temperature

Table 1 Mode frequencies of isolated VO_4 tetrahedra

mode	ν/cm^{-1}	activity[a]
ν_1 (A_1)	826	R
ν_2 (E)	336	R
ν_3 (F_2)	804	R, IR
ν_4 (F_2)	336	R, IR

[a]R, Raman active; IR, IR active.

mode frequencies of this [VO_4] unit have been observed as shown in Table 1. Thus, in $LiNiVO_4$ the high-frequency band located at 821 cm^{-1} corresponds to the stretching mode of the VO_4 tetrahedron which has A_1 symmetry, whereas the band situated at 335 cm^{-1} corresponds to the bending mode of the VO_4 tetrahedron with E symmetry. These vibrations are Raman-active modes. The broadness of the high-frequency band can be tentatively explained in terms of asymmetrical bonding of the VO_4 tetrahedron. Two types of cations, Li and Ni, may be bonded to each oxygen atom of a VO_4 tetrahedron. This introduces some asymmetry in the VO_4 unit without disturbing the overall cubic symmetry of the elementary unit cell. This may occur at the origin of the appearance of additional IR-active modes as well. The bands observed in the 700–850 cm^{-1} region can be attributed to the stretching vibrations of the VO_4 tetrahedron.

A detailed interpretation of the medium-frequency region of Raman and FTIR spectra is difficult because different types of vibrations exist in this spectral domain, involving significant displacement of octahedral and tetrahedral cations simultaneously. Therefore, one may observe either the bending vibrations of the VO_4 tetrahedron or the vibrations involving the octahedral NiO_6, LiO_6 environments. If one considers that all the Li ions are accommodated in octahedral LiO_6 environments, the F_{1u} modes are normally split into (A+2B) Raman-active and IR-active components. Therefore, IR modes having (A+2B) symmetry are intense whereas Raman modes are expected to be very weak. These two modes are observed at 416 and 435 cm^{-1}, respectively. The wavenumbers and the corresponding assignments of the Raman and IR bands of inverse spinel $LiNiVO_4$ are summarized in Table 2.

SEM and EDAX analyses

In general, SEM analysis reveals the nature of the shape, size and surface morphology of the grains with respect to the method and/or conditions of the synthesis. Therefore, we carried out SEM analysis on our final product annealed at 500 °C; the SE micrograph is reproduced in Fig. 8. The photo-

Table 2 Wavenumbers and assignments of the Raman and IR bands of $LiNiVO_4$ (all units are in cm^{-1})

Raman	IR	assignment
335	—	$\nu(VO_4)$
	374	
416		ν(Li—O)
	435	ν(Li—O)
480		ν(Li—O—Ni)
656	651	ν(Li—O—Ni)
790		$\nu(VO_4)$
	815	[antisymmetric stretching]
821		
	852	$\nu(VO_4)$
	905	[symmetric stretching]
908		

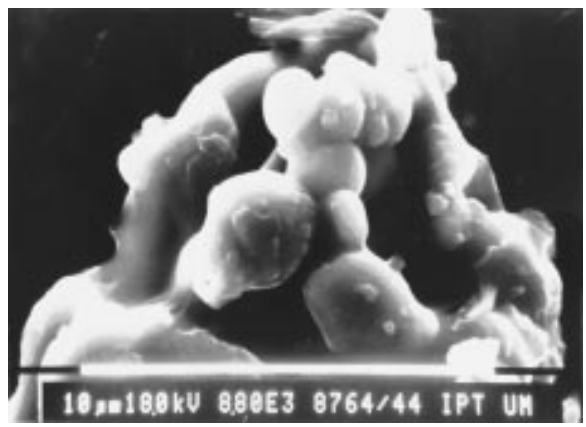

Fig. 8 SE micrograph of inverse spinel $LiNiVO_4$

graph reveals the formation of spherical grains of submicronic nature (average size of grains <1 µm) accompanied by controlled grain growth. Almost all of the grains are well connected with linear grain boundaries and exhibit a nearly pore-free state of the annealed product as seen from the micrograph (Fig. 8). As far as the SEM results are concerned, no such information is available in the literature, according to our knowledge, to compare with our results. However, one cannot expect the above features, such as submicronic grains and pore-free state, in a similar compound prepared *via* solid-state reaction at high temperatures. The aforementioned features are very desirable for a material to be employed as an active electrode material in a modern rechargeable lithium battery.

The elemental analysis of the synthesized product was performed using the EDAX technique. EDAX results were interpreted in terms of the atomic percentage and prove the presence of Ni and V in their stoichiometric proportions. The EDAX technique does not provide any information on lithium.

Thermal analysis

In order to measure the exact phase formation and/or crystallization temperature of the $LiNiVO_4$ samples, DTA and TG measurements were carried out on the precursor powder, recovered before self combustion in the temperature range 30 °C to 450 °C. The DTA and TG curves are shown in Fig. 9. There are three distinguishable changes. The endothermic peak appearing at around 100 °C can obviously be attributed to the removal of water molecules present in the precursor sample. After this step, two exothermic transformations are deduced from the DTA data. The first exothermic process is centred at about 170 °C accompanied by 12% mass loss as deduced from TG analysis. As the process of heating continuing, the mass loss increases, owing to the combustion nature of glycine together with the nitrate and vanadate precursor complexes,

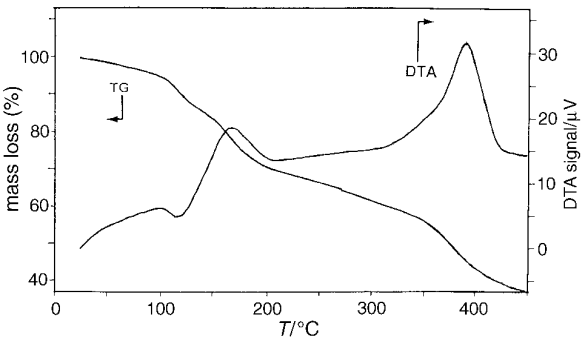

Fig. 9 DTA and TG scans of the precursor complex of $LiNiVO_4$

and results in a second exotherm whose onset begins at 320 °C with a peak maximum at 390 °C accompanied by a huge mass loss of 35%. This indicates that the complex begins to decompose and the exothermic combustion of glycine supplies adequate heat energy for initiating the crystallization of semi-crystalline $LiNiVO_4$. X-Ray diffraction studies substantiate the DTA results. The exotherm occurring at 320 °C presumably indicates the phase formation and/or crystallization of the inverse spinel $LiNiVO_4$.

Electrochemical measurements

The 2450 coin-type electrochemical cells $Li/LiNiVO_4$ and $C/LiNiVO_4$ have been constructed with a newly developed electrolyte composition and the cyclic voltammetric (CV) measurements have been carried out in order to make a quick assessment of the long-term cyclability of the single-phase product, $LiNiVO_4$ as active-cathode material. The cells were cycled between 3.0 and 5.0 V. The cyclic voltammograms reveal the reversible nature of the compound by intercalating/deintercalating Li^+ ions as shown in Fig. 10 and 11. This compound yields a much higher open-circuit voltage of 4.8 V upon removing Li^+. As shown in Fig. 10, the cyclability of these $Li/LiNiVO_4$ cells demonstrates that the capacity degradation is very nominal as exemplified by a small capacity fading occurred over 100 cycles. However, the capacity fading was

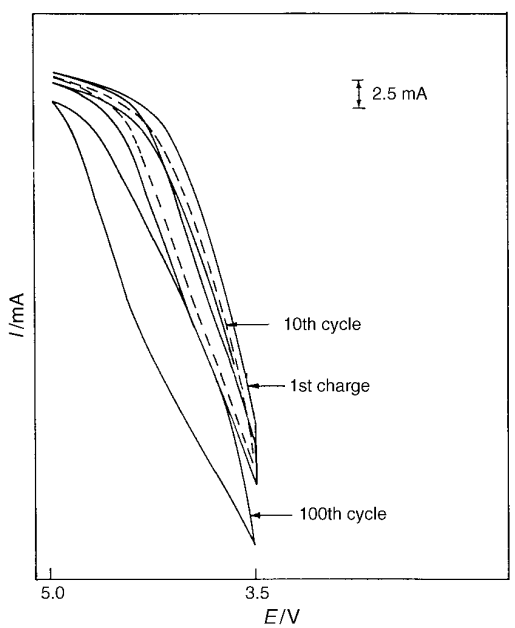

Fig. 10 Cyclic voltammogram of a $Li/LiNiVO_4$ cell employing 1 M $LiPF_6$ in an EC–DMC–MF electrolyte mixture ($T = 28$ °C, scan rate = 10 mV s^{-1})

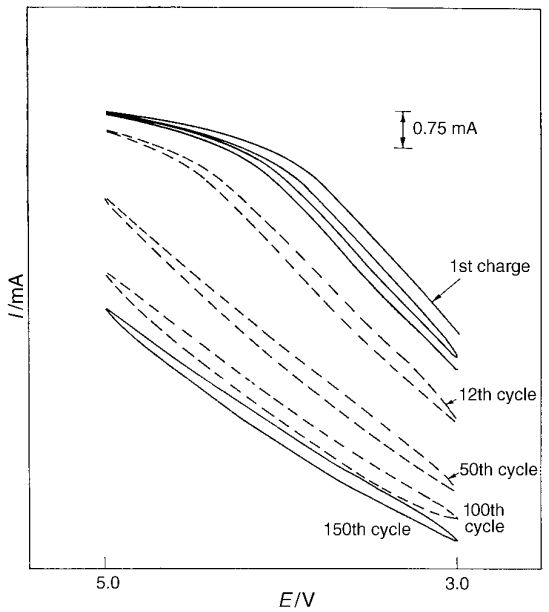

Fig. 11 Cyclic voltammogram of a $C/LiNiVO_4$ cell employing 1 M $LiPF_6$ in an EC–DMC–MF electrolyte mixture ($T = 28$ °C, scan rate = 10 mV s^{-1})

very prominent in the case of the $C/LiNiVO_4$ cell including natural graphite in the carbonaceous anode. Considering the overall capacity, the observed loss in this $C/LiNiVO_4$ cell is presumably due to the irreversible capacity of the graphite anode. Nevertheless, this is considered to be a common feature when employing a carbonaceous material as a Li^+ ion intercalation electrode. The above interesting results encouraged us to throw more light on this inverse spinel powder in lithium batteries. The galvanostatic multiple charge/discharge studies are under progress using an automatic battery cycler and results will be published elsewhere.

Conclusion

This work evolves a new method of low-temperature synthesis, below 350 °C, of electrochemically active novel lithiated metal oxides with high phase purity. The present method yields a single-phase product of the inverse spinel $LiNiVO_4$ as confirmed by XRD measurements. The phase purity of the product was also confirmed from this study with respect to the product obtained from a high-temperature solid-state reaction. The high product yield (>90%) achieved through this method is noteworthy. Thermal analysis proves that the phase formation of the compound occurs at about 320 °C. SEM examination reveals a spherical grain distribution, the average particle size being typically lower than 1 μm. For high-rate cells, the large surface area of the cathode-active material associated with the small particle size is of importance. The evidence for the reversibility emphasizing the deintercalation/intercalation of Li ions from the inverse spinel $LiNiVO_4$ structure was also confirmed by cyclic voltammetry measurements.

The authors wish to express their thanks to IRPA (R&D 03-02-03-0210) for financial assistance. One of us (S.R.S.P.) would like to thank University of Malaya for a Post Doctoral award.

References

1 G. T-K. Fey, W. Li and J. R. Dahn, *J. Electrochem. Soc.*, 1994, **14**, 2279.
2 C. Gonzalez, M. Gaitan, M. L. Lopez, M. L. Veiga, R. Saez-Puche and C. Pico, *J. Mater. Sci.*, 1994, **29**, 3458.

3 J. C. Bernier, P. Poix and A. Michael, *C.R. Acad. Sci.* (*Paris*), 1961, **253**, 1578.
4 S. R. S. Prabaharan, M. S. Michael, T. Premkumar, A. Mani, K. Athinarayanaswamy and R. Gangadharan, *J. Mater. Chem.*, 1995, **5**, 1035.
5 Luis Sanchez, J. Farcy, J-P. Pereira-Ramos, L. Hernan, J. Morales and J. L. Tirado, *J. Mater. Chem.*, 1996, **6**, 37.
6 S. R. S. Prabaharan and M. S. Michael, *Ind. Pat.*, 648/DEL/96, 1996.
7 H. Huang and P. G. Bruce, *J. Electrochem. Soc.*, 1994, **141**, L106.
8 P. Barboux, F. K. Shokoohi and J. M. Tarascon, *US Pat.*, 5 135 732, 1992.
9 S. R. S. Prabaharan, Project Final Report, Department of Science and Technology, New Delhi, India, 1996.
10 (*a*) Joint Commission on Powder Diffraction Standards (JCPDS) card no. 38-1395, International Center for Diffraction Data, Newtown Square, PA, 19073; (*b*) W. Wong, H. McMurdie, B. Paretzkin, C. Hubbard and A. Dragoo, *Powder Diffraction*, 1987, **2**, 262.
11 H. D. Lutz, W. Becker, B. Muller and M. Jung, *J. Raman Spectrosc.*, 1989, **20**, 99.
12 J. Zwinscher, H. C. Gupta and H. D. Lutz, *J. Phys. Chem. Solids*, 1994, **55**, 287.
13 H. D. Lutz, B. Muller and H. J. Steiner, *J. Solid State Chem.*, 1991, **90**, 54.
14 N. Weinstock, H. Schulze and A. Muller, *J. Chem. Phys.*, 1973, **59**, 5063.
15 W. B. White and B. A. De Angelis, *Spectrochim. Acta*, *Part A*, 1967, **23**, 985.

Paper 7/00658F; *Received* 29*th January*, 1997